Role of the 2,6-Bis(trifluoromethyl)phenyl Group on the Acidity of the Corresponding Phosphane[‡]

Karinne Miqueu,[a] Jean-Marc Sotiropoulos,[a] Geneviève Pfister-Guillouzo,*[a]
Valentyn Rudzevich,[b] Vadim Romanenko,[b] and Guy Bertrand[b]

Keywords: Photoelectron spectroscopy / DFT calculations / Phosphanide anions / Phosphanes

The proton affinities of $PhPH^-$ (**1**) and Ar_fPH^- (**2**) were calculated using the B3LYP hybrid functional and the 6-31+G(d,p) basis set. For both anions a net difference was observed. The study of the structural and electronic properties of the anionic species and the corresponding phosphanes $PhPH_2$ (**3**) and Ar_fPH_2 (**4**) allowed us to unsderstand this results and point out the specific role of the 2,6-bis(trifluoromethyl)phenyl (Ar_f) substituent.

Introduction

During the last two decades the 2,6-bis(trifluoromethyl)-phenyl (Ar_f) and 2,4,6-tris(trifluoromethyl)phenyl substituents have been widely used in main-group element chemistry,[2] because they feature a unique combination of steric and electronic properties. The steric effects of perfluoroalkylated aryl groups are well established and highlighted by the synthesis of a wide range of the kinetically stabilized low-coordinated main-group element derivatives, such as phosphaalkenes,[3] diphosphenes,[4] iminoarsanes[5] and their transition metal derivatives. The electronic effects of Ar_f groups are less studied and represent a more recent and developing area.[6]

In a preliminary communication[7] we reported the synthesis and molecular structure of the ion-separated salt $[P(H)Ar_f][K(benzo\text{-}15\text{-}crown\text{-}5)_2]$ representing the first structurally characterized example of a dicoordinated monoorganylphosphanide anion. The use of other bulky substituents (without fluorinated groups) does not allow for the isolation and characterization of such anionic species. Therefore, it was of interest to rationalize this experimental observation and to understand the electronic effects of the Ar_f group. Moreover, information about specific behavior of this latter can be obtained by calculation of the proton affinities of $PhPH^-$ (**1**) and Ar_fPH^- (**2**). This involves naturally the theoretical study of the anions, performed here for the first time, but also the knowledge of the neutral species. The coupling between UV photoelectron spectroscopy and calculations allows us to obtain structural and electronic properties of the phosphanes $PhPH_2$ (**3**) and Ar_fPH_2 (**4**).

For the neutral species, previous works[8] on the basic properties of arylphosphanes had shown that the orientation of the phosphorus lone pair relative to the aromatic ring was an important factor. However, reinvestigating the photoelectron spectrum of $PhPH_2$ (**3**) Veszpremi et al. concluded that the conjugative interaction between the phosphorus lone pair and the phenyl ring is of minor importance in agreement with other spectroscopic and quantum chemical results (MNDO and HF/MP2).[9] The rotational barrier of the phenyl group in **3** has been found to be rather low.

No experimental and theoretical data exist concerning the [2,6-bis(trifluoromethyl)phenyl]phosphane (**4**). Considering the importance of electron correlation for the geometry optimization of compounds having a flat potential energy surface, we investigated the rotational barriers for $PhPH_2$ (**3**) and Ar_fPH_2 (**4**) using the density functional theory. Moreover, the He-I photoelectron spectra of **3** and **4** were carried out and the data compared with the theoretical results. Such an approach would allow to determine if neutral species show notable differences.

First, we are going to present the theoretical results concerning the anionic species and then the PE spectra as well as the calculations of the corresponding phosphanes.

[‡] Application of Photoelectron Spectroscopy to Molecular Properties, 63. Part 62: Ref.[1]

[a] Laboratoire de Chimie-Théorique et Physico-Chimie Moléculaire, CNRS UMR 5624, Université de Pau et des Pays de l'Adour Avenue de l'Université,
B. P. 1155, 64013 Pau cedex, France
Fax: (internat.) + 33-5-59407588
E-mail: genevieve.pfister@univ-pau.fr

[b] UCR-CNRS Joint Research Chemistry Laboratory, UMR 2282, Department of Chemistry, University of California, Riverside, CA 92521-0403, U.S.A.
Fax: (internat.) + 1-909-787-4713
E-mail: gbertran@mail.ucr.edu

DOI: 10.1002/ejic.200300313

Results and Discussion

Anionic Species

The geometrical parameters for the anionic species **1** and **2** are summarized in Table 1. For the two systems $PhPH^-$ (**1**) and Ar_fPH^- (**2**), the lowest energetic form (form **1A** and **2A**, respectively) is planar. The C^1-P-H angle is 95.8° for **1** and 97.5° for **2**. Such a structure presents a lone pair in the C^1PH plane with a strong s character and a pure p orthogonal lone pair. The transition states corresponding to the rotation around the C^1-P bond (form **1B** and **2B**; PH perpendicular to the phenyl ring) are calculated to be 8.76 and 15.52 kcal/mol (ZPE correction) for $PhPH^-$ and Ar_fPH^-, respectively, higher than their minima.

Table 1. Selected bond lengths [Å] and bond angles [°] for the privileged structures and the transition states of $PhPH^-$ (**1**) and Ar_fPH^- (**2**) calculated with the B3LYP hybrid functional and the basis set 6-31+G(d,p)

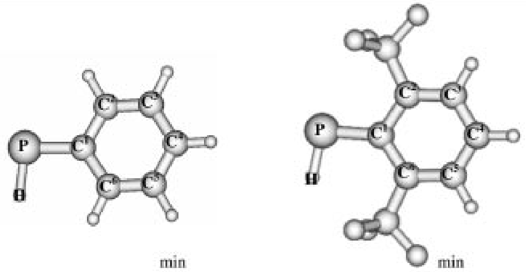

	1A min H–P1–C1–C6 = 0° calcd.	**1B** T.S. H–P1–C1–C6 = 90° calcd.	**2A** min H–P1–C1–C6 = 0° calcd.	 exp.	**2B** T.S. H–P1–C1–C6 = 89.9° calcd.
$P-C^1$	1.811	1.886	1.787	1.795	1.884
C^1-C^2	1.428	1.413	1.459	1.453	1.426
C^2-C^3	1.391	1.400	1.391	1.394	1.401
C^3-C^4	1.406	1.399	1.397	1.392	1.394
C^4-C^5	1.404	1.399	1.395	1.390	1.389
C^5-C^6	1.393	1.400	1.394	1.399	1.405
C^1-C^6	1.427	1.413	1.457	1.452	1.428
$H-P-C^1$	95.82	93.72	97.50	–	95.31
$C^6-C^1-C^2$	114.77	115.76	112.62	113.3	114.24

The stabilization of the planar structure can be explained by the interaction between the π phosphorus lone pair (p character) and the π^*_{b1} orbital of the ring, localized on the C^1 (and C^4) atoms (Figure 1). In fact, for the two minima **1A** and **2A** the HOMO is stabilized by about 0.27 eV for **1** and 0.53 eV for **2**, compared to the transition states **1B** and **2B** (HOMO: n_P^π). In contrast, for the transition states **1B** and **2B** we notice a strong destabilizing of the HOMO-1 (around 0.5 eV), compared to **1A** and **2A** due to an interaction between the s lone pair and the b_1 orbital.

For the fluorinated compound **2**, the inductive effect of the CF_3 groups stabilizes the b_1, a_2, a_2*, and b^*_1 orbitals of the phenyl ring. In this case the destabilizing interaction between the π phosphorus lone pair and the b_1 orbital does not exist and only the stabilizing interaction occurs with the b^*_1. So, the π stabilizing interaction between n_P^π and π^*_{b1} is more important for **2** than for **1** as displayed Figure 1.

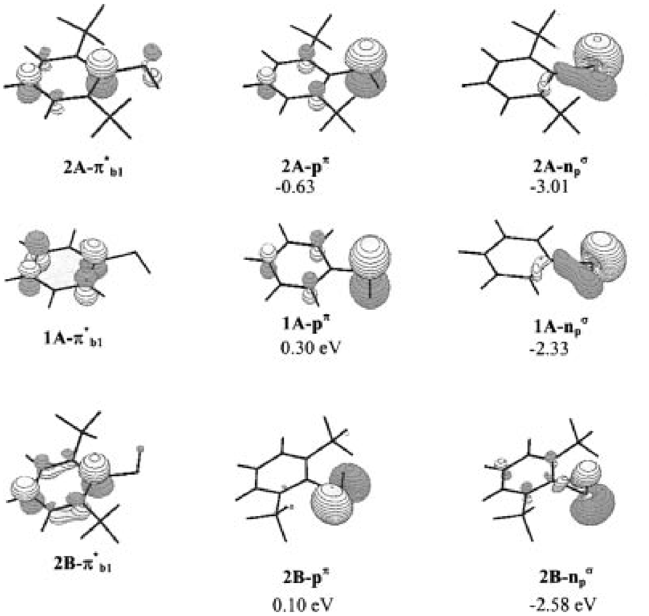

Figure 1. Plot of the molecular orbitals for the minima of $PhPH^-$ (**1A**) and Ar_fPH^- (**2A**) and the corresponding transition states **1B** and **2B**

For the privileged forms **1A** and **2A**, we observe a shortening of the $P-C^1$ bond and a lengthening of the C^1-C^2 and C^1-C^6 bonds compared to the neutral species (Table 2). This effect is more pronounced for **2** than **1** (**2**: $P-C^1$: 1.787 Å, C^1-C^2: 1.459 Å, C^1-C^6: 1.457 Å; **1**: $P-C^1$: 1.811 Å, C^1-C^2: 1.428 Å and C^1-C^6: 1.427 Å). These geometrical changes are due to the stabilizing interaction $n_P^\pi \rightarrow \pi^*_{b1}$. For the anion **2**, these calculated geometric parameters are in particularly good agreement with the X-ray values[7] ($P-C^1$: 1.795 Å, C^1-C^2: 1.453 Å, and C^1-C^6: 1.452 Å). The delocalization of the negative charge (NBO analysis) to the aryl group is well described by the electronic distribution (Table 3). Noteworthy is the π-electronic trans-

Table 2. Selected bond lengths [Å] and bond angles [°] for the privileged structures of $PhPH_2$ (**3A**) and Ar_fPH_2 (**4A**) and their transition states (T.S.) (**3B** and **3C** for $PhPH_2$ and **4B** for Ar_fPH_2), calculated with the B3LYP hybrid functional and the basis set 6-31+G(d,p) (θ = Lp $P-C^1-C^2$ [°]); energetic difference between T.S. and the minimum [kcal/mol]

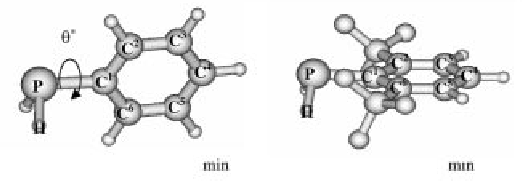

	3A min θ = 10.5°	**3B** T.S. θ = 90°	**3C** T.S. θ = 0°	**4A** min θ = 90°	**4B** T.S. θ = 0°
$P-C^1$	1.856	1.855	1.858	1.876	1.891
C^1-C^2	1.404	1.404	1.403	1.416	1.414
C^2-C^3	1.399	1.397	1.399	1.399	1.400
C^3-C^4	1.396	1.397	1.395	1.390	1.389
C^4-C^5	1.399	1.397	1.399	1.390	1.391
C^5-C^6	1.396	1.397	1.396	1.399	1.399
C^1-C^6	1.405	1.404	1.406	1.416	1.417
$H-P-C^1$	98.11	97.22	97.95	96.70	96.33
$C^6-C^1-C^2$	118.54	118.54	118.55	116.32	116.61
ΣP	288.94	288.26	289.04	287.13	286.22
$E_{T.S.} - E_{min}$	0	0.6	insignifiant	0	1.99

fer of about 0.7 π e^- from the phosphorus lone pair to the π system of the phenyl ring (**1**: 0.62 π e^-; **2**: 0.76 π e^-).[10]

Table 3. NBO charges computed at the B3LYP/6-31G(d,p) level for $PhPH^-$ (**1**) and Ar_fPH^- (**2**)

	$PhPH^-$ (**1A**)	Ar_fPH^- (**2A**)
P	−0.26	−0.09
C^1	−0.32	−0.32
C^2	−0.27	−0.22
C^3	−0.25	−0.20
C^4	−0.33	−0.34
C^5	−0.25	−0.20
C^6	−0.28	−0.23
H^1	−0.08	−0.06

For the transition states **1B** and **2B**, the calculated P−C bonds (1.886 and 1.884 Å, respectively) are longer than those for **1A** and **2A**. The C^1-C^2 and C^1-C^6 bond lengths (ca. 1.427 Å) for **2B** also agree with a weak delocalization of the phosphorus lone pair, with an s character, in the ring as shown in Figure 1.

Thus, considering the charges and the geometric parameters it appears that the phenyl ring substituted by CF_3 groups acts as an electron acceptor by the π^*_{b1} orbital and contributes to the stability of the Ar_fPH^- anion (**2**) which features a quinoid structure.

However, the stabilization of the anion **2** is not the only factor that explains the isolation of such species from the phosphane Ar_fPH_2 precursor **4**. A second reason can be proposed: the presence of the CF_3 groups must induce destabilizing interactions into the neutral molecule. In order to check such a hypothesis, we theoretically determined the stationary points (minima and saddle points) corresponding to the rotation process of the two phosphanes **3** and **4**. In addition, the photoelectron spectra were recorded to determine the possibility of a favored orientation between the aryl group and the phosphorus lone pair. The agreement between theoretical data and PE experiments allow us to determine the importance of interactions between the π system of this aryl group and the n_P phosphorus lone pair.

Phenylphosphane (3)

For the phenylphosphane the energetically privileged rotamer **3A** presents a *gauche* orientation of the phenyl ring ($H^1-P-C^1-C^2$: −112.7°, $H^2-P-C^1-C^2$: 152.9°; Lp $P-C^1-C^2$: 10.5°). In this case, there is a very weak interaction between the π-system of the phenyl ring and the phosphorus lone pair. During the rotation process, two transition states (**3B**; Lp $P-C^1-C^2$: 90°) and (**3C**; Lp $P-C^1-C^2$: 0°) have been found on the potential energy surface. For **3B**, there is a maximal interaction between the phosphorus lone pair and the π system of the phenyl ring, whereas **3C** presents no interaction. The geometrical parameters are described in Table 2. The energy difference between the different transition states (**3B** or **3C**) and the minimum **3A** is very weak (calculated at 0.6 kcal/mol for **3B**) or negligible (for **3C**). It means that a free rotation of the phenyl group in the gas phase can occur. This result is in agreement with the one reported by Veszpremi et al. (HF/MP2 calculations).[9a]

For these different structures the electronic and nuclear repulsion energies are summarized in Table 4. We can note that the lowest energy structure corresponds to a form where the electronic and nuclear repulsion energies are intermediate between those of the two transition states. For **3B**, the electronic and the repulsion energies are strongest, this latter being predominating.

Table 4. Electronic and nuclear repulsion energies [hartrees] for the different structures of $PhPH_2$ (**3**) and Ar_fPH_2 (**4**)

	E_{elec}	E_{rep}
$PhPH_2$ (**3A**) min	−893.013421	318.800771
$PhPH_2$ (**3B**)	−893.206339	318.994787
$PhPH_2$ (**3C**)	−892.953020	318.740385
Ar_fPH_2 (**4A**) min	−2453.638501	1205.321897
Ar_fPH_2 (**4B**)	−2450.487236	1202.174381

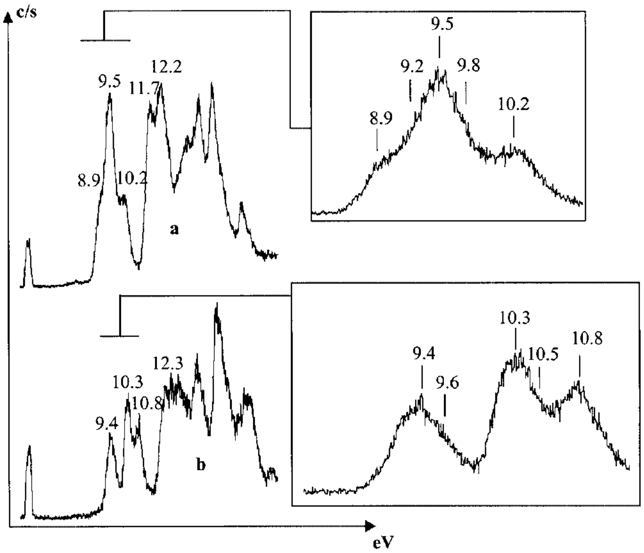

Figure 2. **a**: He-I spectrum of $PhPH_2$ (**3**); **b**: He-I spectrum of Ar_fPH_2 (**4**)

For compound **3**, the PE spectrum (Figure 2) presents, at low energies, three bands of different intensities at 8.9, 9.5 and 10.2 eV, the second one being the most intense.

For the lowest energy structure **3A**, the three first Kohn−Sham (K-S) orbitals are energetically close (Table 5: $\pi_{b1} - n_P$: −6.92; π_{a2}: −7.17; $\pi_{b1} + n_P$: −7.43 eV). Thus, the PE spectrum would present three bands with the same intensities, each separated by about 0.25 eV, or a unique broad band. The experimental spectrum cannot correspond to **3A** since, experimentally, the separation between the first and the third band is about 1.2 eV and the second band is more intense than the first and third ones. This observation suggests the presence of other rotamers. In fact, this PE spectrum would be a superposition of all rotamers' ionizations (Figure 3), as previously observed.[9a]

Table 5. Kohn−Sham energies and ΔSCF values for $PhPH_2$ (minimum **3A** and transition states **3B** and **3C**) and Ar_fPH_2 (minimum **4A** and transition state **4B**) calculated with the B3LYP hybrid functional and the basis set 6-31+G(d,p)

Kohn−Sham energies [eV] (Δ*SCF values*)				
$PhPH_2$ (**3A**)	$PhPH_2$ (**3B**)	$PhPH_2$ (**3C**)	Ar_fPH_2 (**4A**)	Ar_fPH_2 (**4B**)
−6.92	−6.47	−7.13	−7.22	−7.57
$\pi_{b1} - n_P$	$\pi_{b1} - n_P$	π_{a2}	$\pi_{b1} - n_P$	n_P
(*8.86 eV*)	(*8.41 eV*)	(*9.10 eV*)	(*9.14 eV*)	(*9.86 eV*)
−7.17	−7.14	−7.19	−8.25	−8.08
π_{a2}	π_{a2}	π_{b1}	π_{a2}	π_{a2}
−7.43	−7.94	−7.19	−8.67	−8.28
$\pi_{b1} + n_P$	$\pi_{b1} + n_P$	n_p	$\pi_{b1} + n_P$	π_{b1}

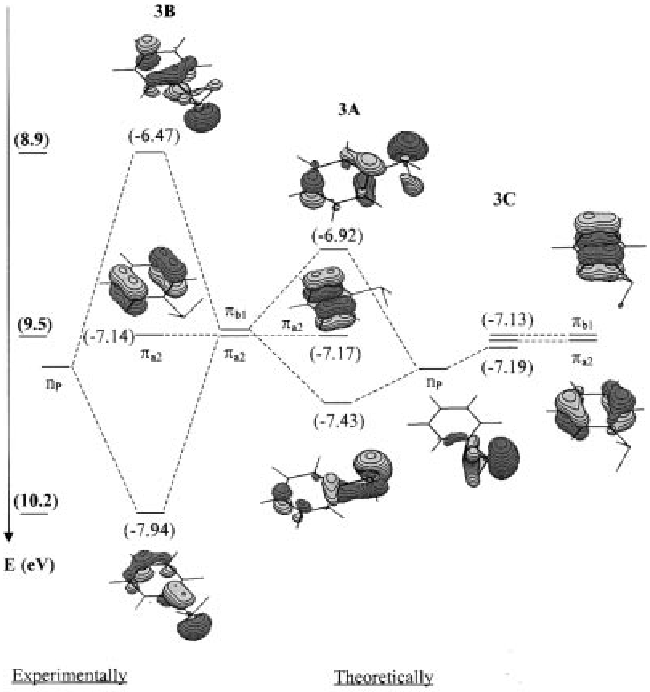

Figure 3. Experimental ionization potentials, molecular orbitals and Kohn−Sham values of $PhPH_2$ (minimum **3A** and transition states **3B** and **3C**)

For **3C** the K-S energies (−7.13: π_{a2}; −7.19 eV: π_{b1} and n_P) of the first three orbitals are almost identical (Table 5). These three ionizations would appear in a unique band, like for **3A**. Taking into account the similar K-S energies for **3A** and **3C** as well as the π_{a2} and π_{b1} ionization potentials of the phenyl ring,[11] the first three ionizations of these two rotamers will be at the same energy (9.5 eV). Thus, the second band can be assigned to the removal of an electron from the $\pi_{b1} - n_P$, π_{a1}, $\pi_{b1} + n_P$ orbitals of **3A** as well as the π_{a2}, π_{b1}, and n_P orbitals of all rotamers around **3C**. This rotamer population explains the intensity of this latter in the PE spectrum.

For **3B**, the first three Kohn−Sham energies (Table 5) are calculated at −6.47: $\pi_{b1} - n_P$; −7.14: π_{a2}; −7.94 eV: $\pi_{b1} + n_P$, respectively. Only the presence of rotamers population with a structure close to **3B** allows the assignment of the complete experimental spectrum. Like for **3A** and **3C**, the second ionization π_{a2} corresponds to the experimental band centered at 9.5 eV. Taking into account the theoretical difference between the first and second ionization (0.67 eV) the band at 8.9 eV corresponds to the removal of an electron from the $\pi_{b1} - n_P$ orbital. Moreover, the comparison between the experimental (1.3 eV) and theoretical (1.4 eV) energetic gap between the first and third band allows us to associate the third ionization to the band at 10.2 eV.

These assignments are consistent with the expanded spectra (Figure 2) where we observe an intense band centered at 9.5 eV with a shoulder between 8.6 and 9.0 eV and a broad shoulder between 9.8 and 10.3 eV.

[2,6-Bis(trifluoromethyl)phenyl]phosphane (4)

For **4**, one minimum is found on the potential energy surface (Table 2). This lowest energy structure (**4A**) corresponds to a maximal interaction between the phosphorus lone pair and the π system. A comparison between **4A** and **3B** (phenyl ring with the same orientation) shows a slight lengthening of the $P-C^1$ bond length (1.876 Å for **4A** and 1.855 Å for **3B**) and a phosphorus pyramidalization more pronounced for **4** (ΣP angle: 287.13° for **4A**, 288.26° for **3B**). An explanation is found considering the strong interatomic and electronic repulsions between the phosphorus lone pair and the CF_3 substituents. For **4A**, the theoretical H−F and P−F distances (2.46 and 2.92 Å, respectively) correspond to a van der Waals contact (2.55 and 3.25 Å, respectively). However, there is a compensation between these high steric repulsions, which destabilize the system and an electronic delocalization between the phosphorus lone pair and the aromatic system, which is stabilizing.

The ring system of the transition state **4B** has similar orientation than **3C** [no interaction between n_P and $\pi_{C=C}$]. It is found to be 1.99 kcal/mol higher in energy than the minimum. As for $PhPH_2$, a free rotation can also be proposed in this case. A lengthening of the $P-C^1$ bond is noteworthy when we compared the calculated geometric parameters of **4B** and **3C** (Table 2).

For these two structures **4A** and **4B** the electronic and nuclear repulsion energies are summarized Table 4. The lowest energy structure **4A** corresponds to the form where the electronic energy is the more important. The presence of σ-attractor CF_3 groups involves an electronic delocalization between the phosphorus lone pair and the aromatic system (π^*_{b1}) which stabilizes the system and counterbalances the high steric interactions (Figure 4). For **4** the photoelectron spectrum (Figure 2) shows three well-separated first bands which appear at 9.4, 10.3, and 10.8 eV, respectively.

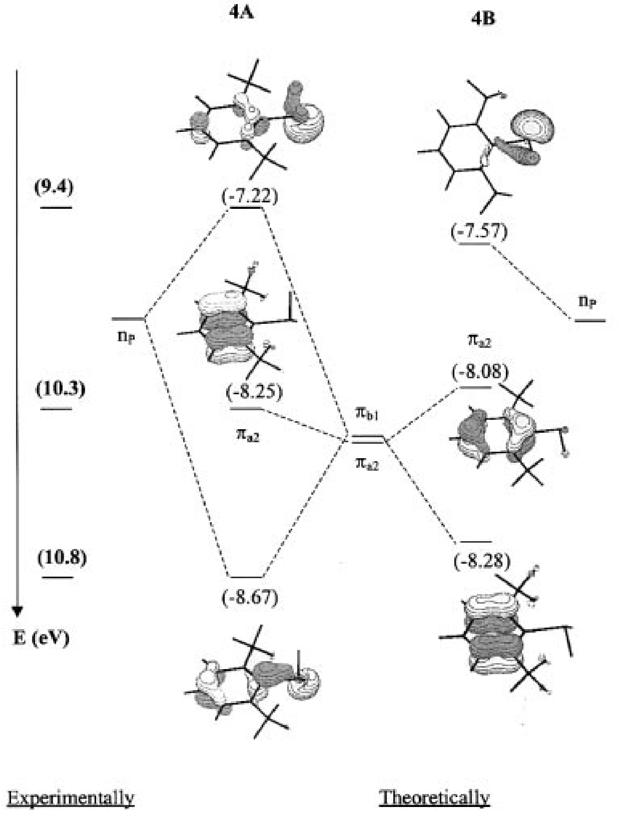

Figure 4. Experimental ionization potentials, molecular orbitals and Kohn−Shan values of Ar_fPH_2 (minimum **4A** and T.S. **4B**)

For the lowest energy structure (**4A**) the three K-S energies (Table 5) are calculated at −7.22: $\pi_{b1} - n_P$; −8.25: π_{a2}; −8.67 eV: $\pi_{b1} + n_P$, respectively. In the PE spectrum the second band, centered at 10.3 eV is associated with the ionization of the π_{a2} orbital.[12] The experimental separation between the first and the third band is about 1.4 eV. Taking into account the calculated energetic gap between the first and third ionizations (1.45 eV), we assign the first band (9.4 eV) to the ionization from the $\pi_{b1} - n_P$ orbital and the third band (10.8 eV) to the $\pi_{b1} + n_P$ orbital.

The weak energy difference between the two rotamers **4A** and **4B**, as previously observed in the case of **1**, involves the existence of a free rotation process. It means that the ionizations of **4B** are going to also appear in the experimental spectrum. For **4B** the K-S energies are the following: −7.57: n_P; −8.08: π_{a2}; −8.28 eV: π_{b1} (Table 5). Thus, for this rotamer, the ionization of the phosphorus lone pair is located in the shoulder of the first band (9.4 eV) and the π_{a2} and π_{b1}' ionizations in the second band centered at 10.3 eV, which explains its intensity. The expanded spectrum allows us to check the existence of a shoulder (9.6 eV) in the first band and the presence of several ionizations near 10.3 eV.

The photoelectron study shows that for these neutral species, the ring orientation is of minor importance.

Proton Affinity

Considering the previous results on the phosphanides and corresponding phosphanes, it was of interest to focus our attention on the proton affinity (PA) of the anion (or the acidity of the phosphane).

Taking into account the equation $A^- + H^+ \rightarrow HA$, PA is the result of the energiy difference between the neutral and the anion species. A net difference is observed between the two anions since PA is calculated at 352.93 kcal/mol for $PhPH^-$ (**1**) and 337.37 kcal/mol for Ar_fPH^- (**2**). Such results are coherent with the existence of the naked phosphanide **2**, both in the solid state and in solution. In fact the Ar_f substituent involves a stabilization of the anion species (interaction $p^\pi \rightarrow \pi^*_{b1}$) but also a destabilization of the corresponding phosphane (important steric repulsion between the phosphorus and fluorine lone pairs). These two factors lead to a peculiar gas-phase acidity for the Ar_fPH_2 compound. It is noteworthy that the gas-phase acidity of **4** is stronger than the one of PH_3 (expt. 370.8 kcal/mol; calcd. 364.7 kcal/mol) and close to the one of HCOOH (found 345 kcal/mol; calcd. 335.5 kcal/mol).

The calculation of the proton affinity can also be performed by the isodesmic reaction $NH_4^+ + Ar_fPH^- \rightarrow Ar_fPH_2 + NH_3$. In this case the PA can reliably be anchored on the experimental value of NH_3 (202.3 kcal/mol[13]). Noteworthy that the PA values resulting from the isodesmic reaction are calculated at 352.0 kcal/mol for **1** and 336.44 kcal/mol for **2**. These latter are very close to the previous ones which result from the energies difference between the neutral and the anion species.

Conclusion

The stabilization of the fluorinated anion Ar_fPH^- (**2**) as well as the presence of destabilizing interactions into the corresponding neutral molecule Ar_fPH_2 (**4**) allow us to explain the difference observed in the calculated proton affinities for **1** and **2**. For the anionic species we theoretically showed that favored form is planar because of stabilizing interaction between the π phosphorus lone pair (p character) and the π^*_{b1} orbital. This latter seems to be more important for the fluorinated compound **2** compared to **1** since the inductive effect of the CF_3 groups involves a stabilization of the a_2, b_1, a^*_2, and b^*_1 orbitals of the aryl group, and decreases the $p^\pi \rightarrow \pi^*_{b1}$ energetic gap. In this case Ar_f is an electron acceptor by its LUMO orbital and contributes to the observed stability of the corresponding anion.

With regard to neutral species, the coupling of UV Photoelectron Spectroscopy and DFT calculations, showed that a free rotation of the aryl group occurs in the gas phase. However, the phosphanes **3** and **4** exhibit different favored forms: the phosphorus lone pair is in maximal interaction with the π system of the ring for **4**, while almost no interaction exists for **3**. For the bulky compound **4**, the orientation of the phenyl ring allows a compensation between two competitive factors: high steric repulsions (between phosphorus and fluorine lone pairs) which destabilize the system and an electronic delocalization between the phosphorus lone pair and the aromatic system, which is stabilizing.

Computational Details

Calculations were performed with the Gaussian 98 program[14,15] using the density functional theory.[16] The various structures were fully optimized at the B3LYP level.[17] This functional is built with Becke's three-parameter exchange functional[17a] and the Lee−Yang−Parr correlation functional.[17c] Kass et al.[18] have shown, with 35 different anionic species, that the density functional theory provides reasonable results concerning acidities compared to the experimental data. Thus, calculations for the anions $PhPH^-$ (**1**) and Ar_fPH^- (**2**) have been carried out using the B3LYP hybrid functional and the 6-31+G(d,p) basis set, with polarization functions on all the atoms and diffuse functions on all non-hydrogen atoms. Moreover, the use of density functional theory (DFT) within its Kohn−Sham (K-S) presents many advantages. First, the cost of a K-S DFT calculation is at most of the same order of magnitude as a Hartree−Fock one whereas most of the description of electron correlation is taken into account. Thus, it is substantially less expensive than traditional correlated techniques. The basis set used for all calculations is the 6-31G+(d,p) set which is augmented with polarisation functions on all the atoms and diffuse functions on all non-hydrogen atoms since the inclusion of polarization is necessary for the obtention of accurate energies. The structures were optimized and the second derivatives were calculated in order to determine if a minimum or a transition state (one negative eigenvalue) existed for the resulting geometry. All total energies have been zero-point energy (ZPE) and temperature corrected using unscaled density functional frequencies. For the large molecules, association between ionization potential and Kohn−Sham (K-S) energies calculated with common functionals (Koopmans' theorem like) has been discussed in depth. Arduengo and co-workers[19] first used DFT calculations at the nonlocal level to assign their photoelectron spectra. They applied a uniform shift to the orbital energies considering the difference between the calculated and experimental molecular ionization potential. The aim was to directly compare the K-S energies to the experimental energies. Moreover, Werstiuk and Rademacher[20] have developed and successfully applied a routine for the interpretation of PE spectra based on B3LYP theory. This routine requires the calculation of the molecule's first vertical ionization potential IP_v. Calculated orbital energies $-\varepsilon$ are then shifted uniformly so that the HOMO energy equals that of the IP_v, giving the higher IPs. More recently, Hoffmann[21] underlined that the K-S orbitals are a good basis for a qualitative interpretation of molecular orbitals. He concludes that if we want to go a step beyond a qualitative interpretation and look at orbital energies as rough ionization potentials and if the DFT calculations are done with commonly used potentials, then it appears we must take the absolute constant and linear orbital energy shift into account by applying a suitable $ax + b$ scaling. In the case of large molecules, the ordering of levels found using the DFT calculations, seems to be qualitatively well translated as well by using HF methods. This fact, despite the evident limits of correlation, gives a good base to discuss the ionizations assignments which cannot be reached by a direct calculation. The "natural population analysis" (NBO calculations) at the given optimized geometries, allowing to calculate orbital populations of molecular wave functions, was carried out according to the Weinhold−Reed partitioning scheme.[22]

Photoelectron Spectra: The photoelectron spectra were recorded with a Helectros 0078 instrument equipped with 127° cylindrical analyser and monitored by a microcomputer supplemented with a digital/analog (D/A) converter. The spectra were calibrated with the known auto-ionisation of helium at 4.98 eV [He-II(He)] and nitrogen ionisation at 15.59 eV.

Acknowledgments

Financial support of this work by the CNRS (France) is gratefully acknowledged. We also thank the Institut du Developpement de Ressources en Informatique Scientifique (IDRIS, Orsay, France), administered by the CNRS, for the calculation facilities, Dr. Gijs Schaftenaar for allowing us to use his graphic program Molden,[23] and the "Societé de Secours des Amis des Sciences" for financial support of K. M.

---

[1] A. Chrostowska, V. Lemierre, T. Pigot, G. Pfister-Guillouzo, I. Saur, K. Miqueu, G. Rima, J. Barrau, *Main Group Met. Chem.* **2002**, *25*, 469.

[2] For a review on this topic see: F. T. Edelmann, *Comments Inorg. Chem.* **1992**, *12*, 259.

[3] K. B. Dillon, H. P. Goodwin, *J. Organomet. Chem.* **1994**, *469*, 125.

[4] [4a] K. B. Dillon, H. P. Goodwin, *J. Organomet. Chem.* **1992**, *429*, 169. [4b] K. B. Dillon, V. C. Gibson, L. I. Sequeira, *J. Chem. Soc., Chem. Commun.* **1995**, 2429. [4c] K. B. Dillon, V. C. Gibson, J. A. K. Howard, L. I. Sequeira, J. W. Yao, *Polyhedron* **1996**, *15*, 4173.

[5] J.-Th. Ahlemann, A. Künzel, H. W. Roesky, M. Noltemeyer, L. Markovskii, H. G. Schmidt, *Inorg. Chem.* **1996**, *35*, 6644.

[6] [6a] M. G. Davidson, K. B. Dillon, J. A. K. Howard, S. Lamb, M. D. Roden, *J. Organomet. Chem.* **1998**, *550*, 481. [6b] J. E. Bender IV, M. M. Banaszak Holl, J. W. Kampf, *Organometallics* **1997**, *16*, 2743. [6c] J. E. Bender IV, A. J. Shusterman, M. M. Banaszak Holl, J. W. Kampf, *Organometallics* **1999**, *18*, 1547. [6d] N. Burford, Ch. L. B. Macdonald, D. J. LeBlanc, T. S. Cameron, *Organometallics* **2000**, *19*, 152. [6e] G. M. Benedikt, B. L. Goodall, S. Iyer, L. H. McIntosh III, R. Mimna, L. F. Rhodes, C. S. Day, V. W. Day, *Organometallics* **2001**, *20*, 2565.

[7] L-V. Rudzevich, H. Gornitzka, V-D. Romanenko, G. Bertrand, K. Miqueu, J-M. Sotiropoulos, G. Pfister-Guillouzo, *Angew. Chem. Int. Ed.* **2001**, *41*, 7, 1193.

[8] [8a] S. Ikuta, P. Kebarle, *Can. J. Chem.* **1983**, *61*, 97. [8b] S. T. Howard, J. A. Platts, *J. Phys. Chem.* **1995**, *99*, 9027. [8c] S. T. Howard, J. P. Foreman, P. G. Edwards, *Inorg. Chem.* **1996**, *35*, 5812.

[9] [9a] L. Nyulaszi, D. Szieberth, G. I. Csonka, J. Reffy, J. Heinicke, T. Veszpremi, *Struct. Chem.* **1995**, *6*, 1. [9b] D. E. Cabelli, A. H. Cowley, M. J. S. Dewar, *J. Am. Chem. Soc.* **1981**, *103*, 3286. [9c] D. E. Cabelli, A. H. Cowley, M. J. S. Dewar, *J. Am. Chem. Soc.* **1981**, *103*, 3290.

[10] These charges are computed with B3LYP/6-31G(d,p).

[11] Experimentally, the π ionizations (π_{b1}, π_{a1}) of the phenyl ring appear at 9.24 eV.[24] Theoretically the K-S energies of the π ionizations are -7.01 eV.

[12] For $Ph(CF_3)_2$ the experimental π_{a2} and π_{b1} ionization potentials are 10.41 eV.

[13] [13a] R. Yamdagni, P. Kebarle, *J. Am. Chem. Soc.* **1973**, *95*, 3504. [13b] R. Yamdagni, P. Kebarle, *J. Am. Chem. Soc.* **1976**, *98*, 1320. [13c] J. F. Wolf, R. H. Staley, I. Koppel, M. Taagepera, R. T. Mciver, J. L. Beauchamp, R. W. Taft, *J. Am. Chem. Soc.* **1977**, *99*, 5417.

[14] M. J. Frisch, G. W. Trucks, H. B. Schlegel, G. E. Scuseria, M. A. Robb, J. R. Cheeseman, V. G. Zakrzewski, J. A. Montgomery, R. E. Stratman, J. C. Burant, S. Dapprich, J. M. Millam, A. D. Daniels, K. N. Kudin, M. C. Strain, O. Farkas, J. Tomasi, V. Barone, M. Cossi, R. Cammi, B. Mennucci, C. Pomelli, C. Adamo, S. Clifford, J. Ochterski, G. A. Petersson, P. Y. Ayala, Q. Cui, K. Morokuma, D. K. Malick, A. D. Rabuck, K. Raghavachari, J. B. Foresman, J. Cioslowswi, J. V. Ortiz, A. G. Baboul, B. B. Stefanov, G. Liu, A. Liashenko, P. Piskorz, I. Komaromi, R. Gomperts, R. Martin, D. J. Fox, T. Keith, M. A. Al-Laham, C. Y. Peng, A. Nanayakkara, C. Gonzalez, M. Challacombe, P. M. W. Gill, B. Jonhson, W. Chen, M. W. Wong, J. L. Andres, M. Head-Gordon, E. S. Replogle, J. A. Pople, *Gaussian 98*, Revision A.7, Gaussian, Inc., Pittsburgh PA, **1998**.

[15] W. J. Hehre, L. Radom, P. v. R. Schleyer, J. A. Pople, *Ab Initio Molecular Orbital Theory*, John Wiley and Sons, New York, **1986**.

[16] R. G. Parr, W. Yang, *Functional Theory of Atoms and Molecules* (Eds.: R. Breslow, J. B. Goodenough), Oxford University Press, New York, **1989**.

[17] [17a] A. D. Becke, *Phys. Rev.* **1988**, *A38*, 3098. [17b] A. D. Becke, *J. Chem. Phys.* **1993**, *98*, 5648. [17c] C. Lee, W. Yang, R. G. Parr, *Phys. Rev.* **1988**, *B37*, 785.

[18] G. N. Merill, S. R. Kass, *J. Phys. Chem.* **1996**, *100*, 17465.

[19] A. J. Arduengo III, H. Bock, H. Chen, M. Denk, D. A. Dixon, J. C. Green, W. A. Hermann, N. L. Jones, M. Wagner, R. West, *J. Am. Chem. Soc.* **1994**, *116*, 6641.

[20] [20a] H. M. Muchall, P. Rademacher, *J. Mol. Struct.* **1997**, *435*, 157. [20b] H. M. Muchall, P. Rademacher, *J. Mol. Struct.* **1998**, *471*, 189. [20c] H. M. Muchall, N. H. Werstiuk, B. Choudhurry, *Can. J. Chem.* **1998**, *76*, 221. [20d] H. M. Muchall, N. H. Werstiuk, B. Choudhurry, J. Ma, J. Warkentin, J. P. Pezacki, *Can. J. Chem.* **1998**, *76*, 238.

[21] R. Stowasser, R. Hoffmann, *J. Am. Chem. Soc.* **1999**, *121*, 3414.

[22] [22a] A. E. Reed, L. A. Curtiss, F. Weinhold, *J. Chem. Rev.* **1988**, *88*, 899. [22b] J. P. Foster, F. Weinhold, *J. Am. Chem. Soc.* **1980**, *102*, 7211.

[23] G. Schaftenaar, J. H. J. Noordik, *Comput.-Aided Mol. Des.* **2000**, *14*, 123.

[24] K. Kimura, S. Katsumata, Y. Achiba, T. Yamazaki, S. Iwata, *Handbook of He I Photoelectron Spectroscopy of Fundamental Organic Molecules*, Japan Scientific Societies Press, Tokyo, Japan, **1981**.

Received May 27, 2003